Quantitative Evaluation of Solidication Brittleness of Weld Metal during Solidification by In-Situ Observation and Measurement (Report III)†

– Effect of Strain Rate on Minimum Ductility Required for Solidification Crack Initiation in Carbon Steels, Stainless Steels and Inconel Alloy –

Fukuhisa MATSUDA*, Hiroji NAKAGAWA**, Shogo TOMITA***

Abstract

Initiation condition of weld solidification cracking in relation to strain rate is analyzed by direct observation technique MISO for plain carbon steels, stainless steels and so on. All the materials used show a dependency of the minimum dutility required for crack initiation on strain rate. Namely, the minimum ductility is lowered with a decrease in strain rate. The tendency is noticeable in materials of low crack susceptibility. Therefore, for the comparison of crack susceptibilities among materials the minimum ductility measured under a high strain rate is better than that under a low strain rate. On the other hand, the strain rate in the self-restraint cracking test and perhaps also in welding the fabrication is shown to be so low that the difference of the minimum ductility among materials is little. Under such low strain rate, the lower critical strain rate below which the crack can not occur is excellent for the comparison of crack susceptibilities.

KEY WORDS: (Solidification) (Hot Cracking) (Carbon Steels) (Stainless Steels) (Welding)

1. Introduction

It is well known that the Varestraint test is excellent and has good reproducibility for the evaluation of solidification crack susceptibility, and thus widely used. However, it is pointed out[1] that the susceptibility of commercial Al-Mg alloy evaluated by the Varestraint test is too high and does not coincide with that known in welding fabrication. Concerning this problem, one of the authors revealed that this discrepancy may be eliminated by adopting slow bending speed in the Varestraint test.[2] This suggests that the solidification crack susceptibility is strain rate-depending phenomena. This dependency is also suggested a little in the study[3] on weld solidification crack in fully austenitic stainless steel. Generally, the dependency of ductility on strain rate is well known fact in the field of hot workability and creep, and is also clearly seen in the ductility-dip cracking in welding Fe-36%Ni alloy.[4] The study on this dependency in solidification cracking has not been done until now, because there has been no technique to measure and analyze it in detail.

In recent years, the authors have established the availability of the MISO technique[5] by which the ductility of solidifying weld metal is evaluated by film analysis after direct photographing the cracking phenomenon during welding. By utilizing the MISO technique, the ductilities of solidifying fully austenitic stainless steel and aluminum alloys that are generally too low to be evaluated in the Varestraint test[1,3] could be well evaluated.[6] Therefore, the authors have intended to evaluate the dependency of solidifying weld metal on strain rate by the MISO technique combined with a tensile cracking tester that is capable of changing crosshead speed. Moreover, the strain rate in selfrestraint cracking test is evaluated by experiment and calculation for the order estimation of that in welding fabrication.

2. Materials Used and Experimental Methods

2.1 Materials

The chemical composition of tentative plain carbon steels, commercial stainless steels and Inconel alloy used in tensile hot cracking test are shown in **Table 1(a)**, and ones of commercial plain carbon steels used in Houldcroft-type cracking test are shown in **Table 1(b)**. The carbon content of the tentative plain carbon steels was varied from about 0.02 to 0.55%, and the sulphur or phosphorus content was increased to about 0.02–0.03% in those of carbon levels 0.02, 0.04 and 0.15% in addition to the low level sulphur and phosphorus.

2.2 Tensile hot cracking test

The MISO technique was combined with a tensile hot cracking tester that has the capacity of 29.4 kN and has

† Received on November 5, 1986
* Professor
** Research Instructor
*** Graduate Student of Osaka Univ.

Transactions of JWRI is published by Welding Research Institute of Osaka University, Ibaraki, Osaka 567, Japan

Table 1 Chemical compositions of materials used

(a) Tentative plain carbon steels, stainless steels and Inconel alloy used for tensile hot cracking test

Material	Item	Chemical composition (wt%)										
		C	Si	Mn	P	S	Ni	Cr	Mo	Al*	N	O
Plain carbon steel	C023	0.023	0.130	0.966	0.0040	0.0050	-	-	-	0.002	0.0018	0.0044
	C024	0.024	0.148	0.900	0.0052	0.0049	-	-	-	0.004	0.0011	0.0026
	C04	0.038	0.147	0.905	0.0051	0.0045	-	-	-	0.002	0.0014	0.0048
	C06	0.060	0.152	0.979	0.0038	0.0050	-	-	-	0.003	0.0019	0.0047
	C09	0.093	0.145	0.975	0.0043	0.0050	-	-	-	0.008	0.0015	0.0025
	C12	0.118	0.153	1.008	0.0032	0.0061	-	-	-	0.006	0.0008	0.0019
	C15	0.145	0.144	0.968	0.0039	0.0050	-	-	-	0.009	0.0013	0.0013
	C20	0.214	0.193	0.976	0.0046	0.0060	-	-	-	0.004	0.0010	0.0046
	C30	0.322	0.139	0.984	0.0044	0.0060	-	-	-	0.005	0.0019	0.0031
	C40	0.412	0.193	0.975	0.0040	0.0061	-	-	-	0.006	0.0012	0.0019
	C50	0.543	0.148	0.971	0.0054	0.0060	-	-	-	0.008	0.0020	0.0024
	C02-S	0.021	0.145	0.962	0.0047	0.0280	-	-	-	0.003	0.0016	0.0031
	C02-P	0.015	0.167	0.971	0.0221	0.0040	-	-	-	-	0.0016	0.0031
	C04-S	0.036	0.149	0.896	0.0047	0.0199	-	-	-	0.003	0.0011	0.0030
	C04-P	0.040	0.168	0.981	0.0218	0.0058	-	-	-	0.002	0.0012	0.0067
	C15-S	0.143	0.145	0.968	0.0038	0.0220	-	-	-	0.012	0.0009	0.0023
	C15-P	0.144	0.172	0.971	0.0219	0.0050	-	-	-	-	0.0016	0.0019
	C40-P	0.398	0.195	0.974	0.0215	0.0059	-	-	-	0.003	0.0014	0.0024
Stainless steel	SUS304L	0.02	0.59	0.99	0.028	0.013	9.75	19.09	0.08	-	-	-
	SUS430	0.06	0.33	0.70	0.028	0.008	0.09	15.92	-	-	-	-
	SUS310S	0.07	0.80	1.55	0.016	0.005	20.08	25.00	0.10	-	-	-
Inconel alloy	Inconel 600	0.003	0.28	0.33	0.005	0.002	-	15.37	-	-	-	-

*Soluble

(b) Commercial carbon steels used for Houldcroft-type cracking test

Material	Item	Chemical composition (wt%)				
		C	Si	Mn	P	S
Plain carbon steel	SS41	0.06	0.01	0.31	0.017	0.021
	S35C	0.34	0.02	0.77	0.023	0.017
	S45C	0.45	0.28	0.62	0.035	0.040
	SK6	0.77	0.28	0.43	0.020	0.009

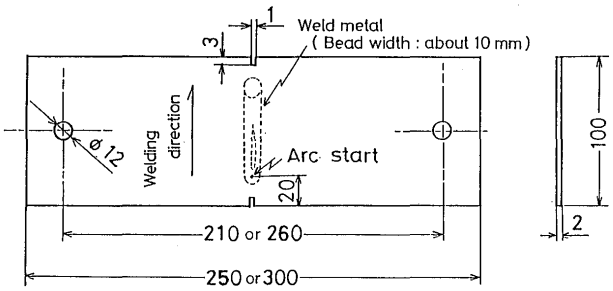

Fig. 1 Shape and size of specimen used for tensile hot cracking test

two movable chuck to fix the photographed position.

The shape and the size of the specimens used are shown in **Fig. 1**. GTA welding was used without filler metal in conditions of 70A, 12V (DCEN), 50 mm/min. Tensile deformation was applied perpendicular to the welding direction during the welding with the tensile hot cracking tester under various crosshead speed (C.H.S.). Crosshead speed (C.H.S.) selected were 20, 2 and proper one between 0.06 and 0.45 mm/sec. Crosshead speed (C.H.S.) of 20 mm/sec was the maximum in the tester used and available to evaluate solidification brittleness temperature range (BTR) because the move of solidification front during the deformation could be nearly ignored. Crosshead speed (C.H.S.) between 0.06 and 0.45 mm/sec was used to evaluate the critical minimum ductility and critical strain rate required for crack initiation, which will be mentioned later.

The behaviors of crack initiation and propagation were photographed by high speed cinecamera. The arrangement of the equipments was explained elsewhere.[1)]

2.3 Houldcroft-type cracking test

Houldcroft-type cracking test was used to assess the strain rate in welding fabrication. The shape and the size of the specimens used are shown in **Fig. 2**. The size of the specimen and the slit length were varied as shown in the list in Fig. 2 to change the extent of rotational deformation. Judging from the effects of specimen size and slit length,[7)] it was expected that the rotational deformation rate increased with the decrease in specimen size or increase in slit length. GTA welding was done without filler metal under the conditions of 50A, 12V (DCEN), 50 mm/min. Initiation and propagation of solidification cracking were photographed by high speed cine camera. Moreover,

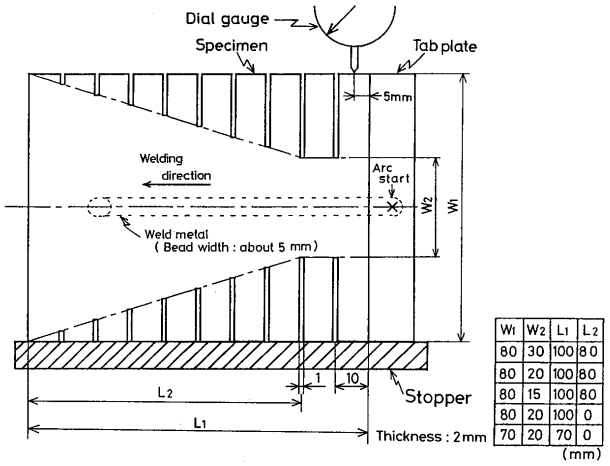

W1	W2	L1	L2
80	30	100	80
80	20	100	80
80	15	100	80
80	20	100	0
70	20	70	0

Fig. 2 Shape and size of specimen used for Houldcroft-type cracking test

the rotational deformation rate near the end of the specimen was also measured by dial gauge as shown in Fig. 2 to evaluate the effect of gauge length on the strain rate measured.

2.4 Measuring method of strain and strain rate

2.4.1 General measuring method of strain and strain rate

In picture analysis, as mentioned in the previous paper,[1] the reference points for gauge length to measure the strain were chosen from many natural spotty marks on the surface of weld metal. There are two kinds of measuring methods of strain and strain rate depending on C.H.S. as shown in **Fig. 3** and **Fig. 4**.

Figure 3 corresponds to the case of high C.H.S., where the tensile deformation is applied after the reference points moved a little from the solidification front. Namely, the reference points of span l_0 are located at solidification front at $t_s = 0$ as shown in (a), and the rapid tensile deformation is applied when the span is l_1 at $t_s = t_1$ as shown in (b). Now, it should be noticed that the time t_1 is not predetermined, but depends on material under constant welding condition. In other words, the tensile deformation is applied at will around the time when the welding arc passes the middle of the specimen width, and the time t_1 is measured by film analysis. Then, crack is initiated when the span is l_2 at $t_s = t_2$ as shown in (c). Between $t_s = 0$ and t_1, the specimen undergoes free contraction or restraint by two chucks. It was already confirmed[1] that the change in the span l_1-l_0 is very small, one of the example will be shown in Fig. 7. Therefore, the minimum ductility required for crack initiation, ϵ_i, can be calculated by Eq. (1) or (1)'.

$$\epsilon_i = \frac{l_2 - l_1}{l_1} \times 100\,(\%) \qquad (1)$$

$$\fallingdotseq \frac{l_2 - l_0}{l_0} \times 100\,(\%) \qquad (1)'$$

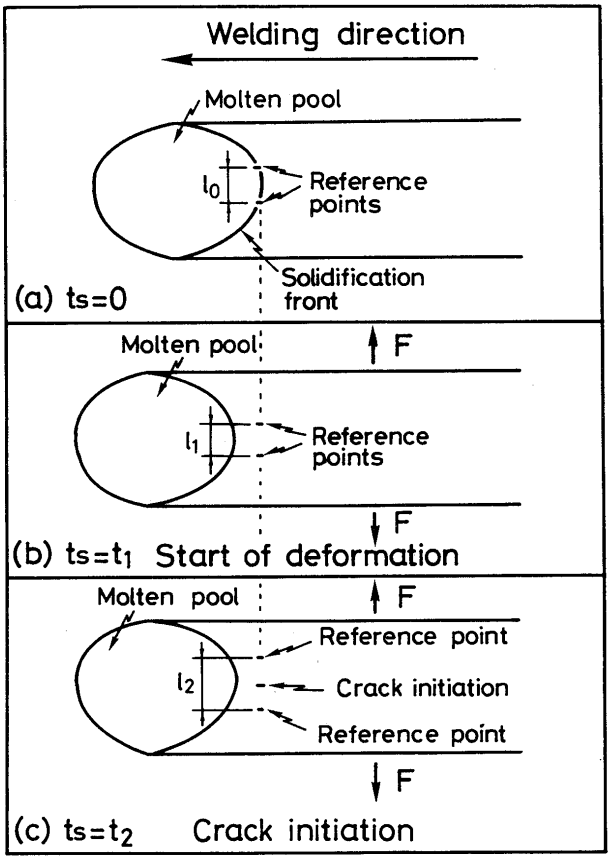

Fig. 3 Measuring principle of strain and strain rate by means of MISO, C.H.S. = high

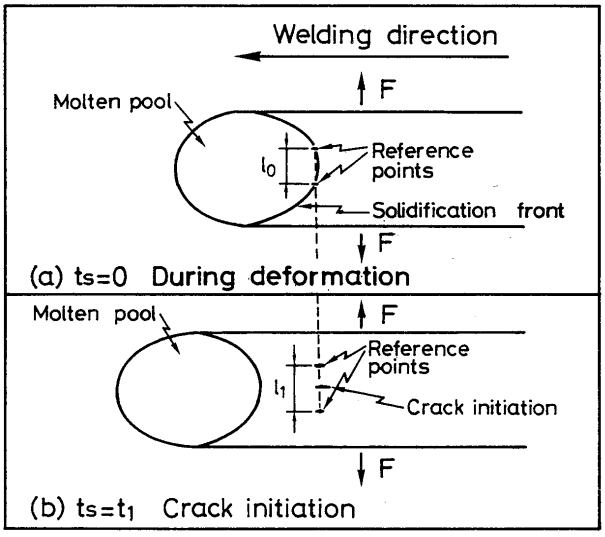

Fig. 4 Measuring principle of strain and strain rate by means of MISO, C.H.S. = low

The strain rate, $\dot{\epsilon}_i$, can be represented by Eq. (2).

$$\dot{\epsilon}_i = \frac{\epsilon_i}{t_2 - t_1} \quad (\%/\text{sec}) \qquad (2)$$

Figure 4 corresponds to the case of slow C.H.S., where the location of reference points are deformed continuously from the solidification front to the crack initia-

tion site. Referring to the designations in Fig. 4, ϵ_i and $\dot{\epsilon}_i$ can be easily represented by Eqs. (3) and (4)

$$\epsilon_i = \frac{l_1 - l_0}{l_0} \times 100\ (\%) \qquad (3)$$

$$\dot{\epsilon}_i = \epsilon_i / t_1 \qquad (\%/\text{sec}) \qquad (4)$$

In each case, the span of the reference points, namely the gauge length selected was 0.9 to 1.7 mm.[1)]

2.4.2 The measuring method of critical minimum ductility and critical strain rate required for crack initiation

As mentioned later, low strain rate is general in welding fabrication. Therefore, lower critical strain rate below which solidification crack cannot occur and the minimum ductility at this critical strain rate are important. In principle several tests under different C.H.S. are required in order to evaluate the critical strain rate. Fortunately, however, only a few specimens were enough, because the strain rate just behind the solidification front was gradually increased with lapse time after the start of deformation during welding under constant C.H.S. One of the example will be shown later in Fig. 6. The reason for this gradual increase in strain rate is thought to be strain accumulation to the hot region behind the molten pool.[1)] Proper selection of C.H.S. between 0.06 and 0.45 mm/sec mentioned in 2.2 yielded efficient evaluation of the critical strain rate.

3. Experimental Results and Discussions

3.1 Effect of strain rate on minimum ductility

3.1.1 Minimum ductility in rapid tensile test

Figure 5 shows the ductility curves of three tentative plain carbon steels under C.H.S. of 20 mm/sec. Solid mark indicates the crack initiation temperature and the minimum ductility required for crack initiation. This minimum ductility is designated as ϵ_{iR}, because it was measured by rapid C.H.S. The strain during crack propagation was measured by the Moving Gauge Method mentioned in the previous paper.[1)] The temperature range enclosed by the ductility curve means the solidification brittleness temperature range (BTR).

3.1.2 Minimum ductility in critically slow tensile test

Figure 6 shows an example of gradual increase in strain rate behind the solidification front together with lapse time under C.H.S. of 0.2 mm/sec. The abscissa means the lapse time t_s in which the reference points moved from the solidification front, having the same definition as that in Figs. 3 and 4. The lapse time τ inside Fig. 6 is defined as the time from the start of tensile deformation. It should be noticed that the gradient of increasing strain,

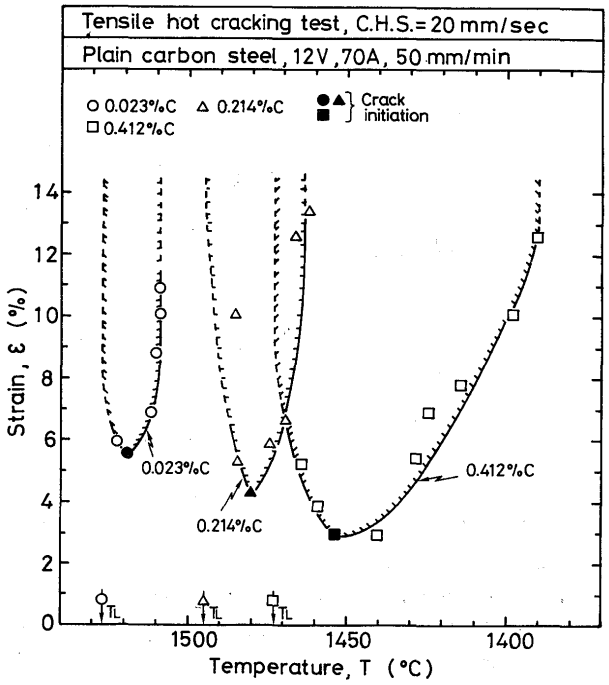

Fig. 5 Examples of ductility curves of tentative plain carbon steels, the minimum of which gives ϵ_{iR}

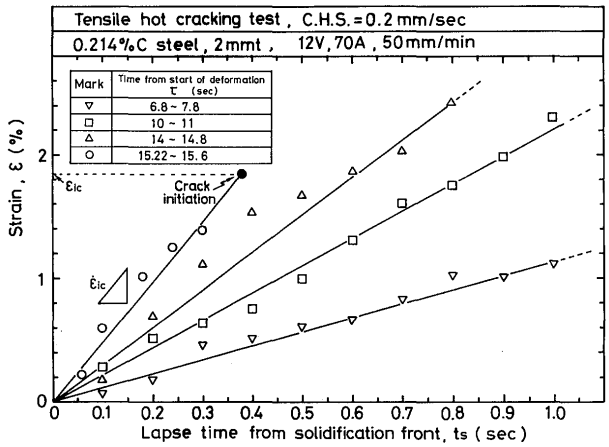

Fig. 6 An example of gradual increase in strain rate behind the solidification front together with lapse time after the start of welding under C.H.S. = 0.2 mm/sec

namely, the strain rate increased gradually together with τ, and crack was initiated at solid mark. Therefore, the ordinate value of the solid mark and the gradient of the line connecting the origin to the solid mark give the critical minimum ductility (ϵ_{ic}) and the critical strain rate ($\dot{\epsilon}_{ic}$), respectively.

3.1.3 Comparison of minimum ductility under different C.H.S.

Figure 7 compares the strain increment during testing and the minimum ductility under three C.H.S. The meaning of ϵ_{iR} was mentioned in 3.1.1, and the behavior of square mark between t_s from 0 to about 0.2 sec confirms that the strain is almost constantly zero before the application of tensile deformation as mentioned in 2.4.1. The meaning of ϵ_{ic} was mentioned in 3.1.2. The minimum

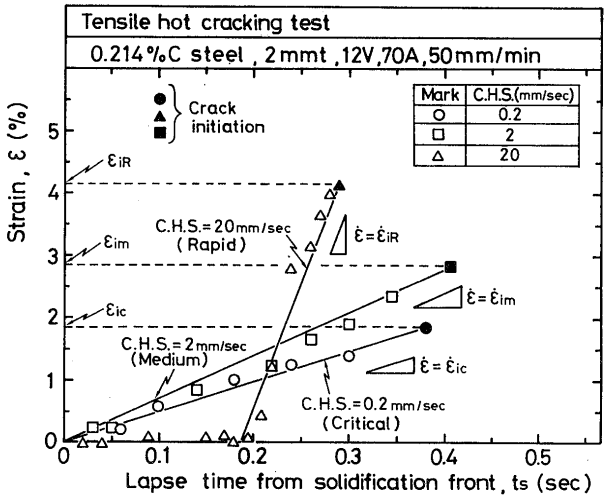

Fig. 7 Comparison of strain increment and minimum ductility in different C.H.S., giving strain-rate dependency of minimum ductility

ductility measured under C.H.S. of 2 mm/sec is designated as ϵ_{im} because this C.H.S. is medium between the former two C.H.S. Comparison of these three indicates clearly the dependency of minimum ductility on strain rate. Namely, the minimum ductility decreases with the decrease in strain rate.

3.1.4 Strain-rate dependency of minimum ductility in carbon steel

Figure 8 summarized the relation between strain rate and the minimum ductility for several tentative plain carbon steels. In every case the minimum ductility increases together with strain rate. It is noticed that the dependency of the minimum ductility on strain rate is remarkable in low carbon steel containing low S and P.

One may suppose that the difference extent of strain-rate dependency is affected by solidifying phase, namely

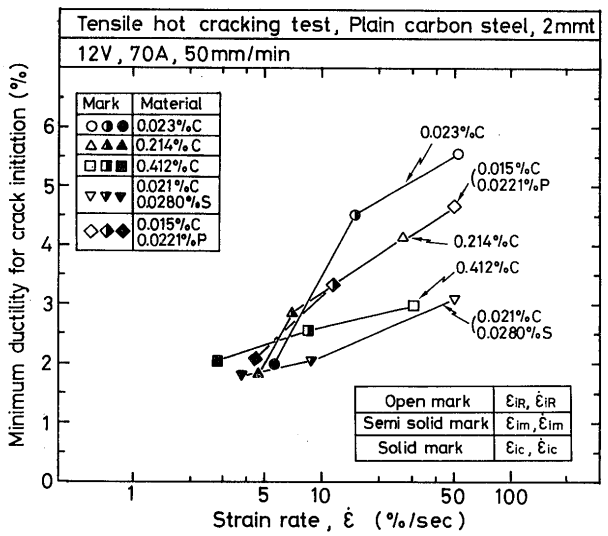

Fig. 8 Effect of carbon, sulphur and phosphorus on strain-rate dependency of minimum ductility in plain carbon steel

primary ferrite or austenite, because there seems to be a possibility that the higher flow stress and the lower rate of dynamic recovery[8] during hot working and the higher impurity segregation during solidification in austenite phase comparing those in ferrite phase would affect the ductility. However, it may be denied as follows. Namely, it is noticed that the strain-rate dependency of 0.021% carbon steel containing 0.0280% sulphur is as little as that of 0.412% carbon steel. It is well known that both carbon and sulphur increases the crack susceptibility and that sulphur has little effect on solidifying phase. Therefore, it may be concluded that this strain-rate dependency is noticeable in low susceptible materials. This tendency is also confirmed by the comparison between 0.023% carbon steel and 0.015% carbon steel containing 0.0221% phosphorus.

This behavior is represented in relation to carbon content in **Fig. 9**, where C.H.S., sulphur and phosphorus contents are used as parameters. It is worthy of note that ϵ_{iR} is most sensitive to compare the crack susceptibility among materials and that ϵ_{ic} is almost constant for all materials including high sulphur or high phosphorus materials, although the constant characteristic of ϵ_{ic} is not thought to be inevitable.

3.1.5 Strain-rate dependency of minimum ductility in stainless steel

The relation between strain rate and the minimum ductility in 304L, 430 and 310S stainless steels and Inconel alloy 600 is shown in **Fig. 10**. The similar strain-rate dependency is seen in all materials. The dependency is noticeable in 304L and 430 stainless steels, but is not noticeable in 310S and Inconel alloy 600. It is well known that 304L and 430 stainless steel has fairly low crack susceptibility in contrast with 310S and Inconel alloy 600. Therefore, it may be also concluded that the strain-rate dependency is noticeable in the materials of low crack susceptibility.

Figure 11 compares ϵ_{iR}, ϵ_{im} and ϵ_{ic} among these materials, where the materials are arranged in the order

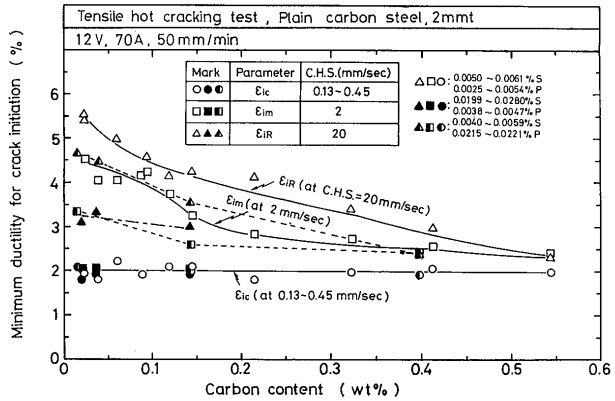

Fig. 9 Effect of carbon content on minimum ductility under different C.H.S.

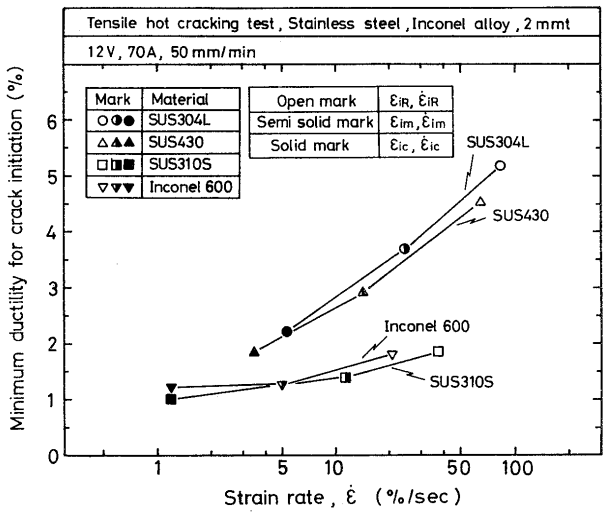

Fig. 10 Strain-rate dependency of minimum ductility in stainless steels and Inconel alloy 600

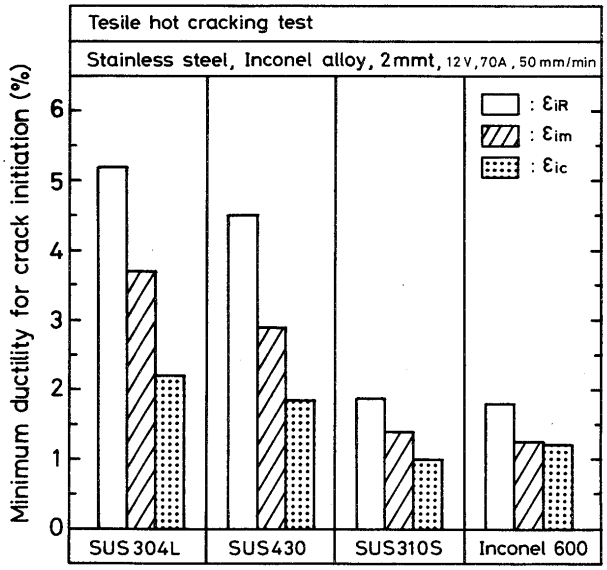

Fig. 11 Comparison of minimum ductility in different C.H.S. in stainless steels and Inconel alloy 600

accepted usually. Similarly in carbon steels in Fig. 9, ϵ_{iR} is most sensitive and ϵ_{ic} is most insensitive for the evaluation of crack susceptibility.

3.2 Characteristics of Critical Strain Rate in low tensile condition

The results in 3.1 show that ϵ_{ic} evaluated in the critical strain rate is not sensitive for the comparison of susceptibilities among materials, although it will be mentioned in next section that the strain rates in welding fabrication are nearly in the same order of the critical strain rate. Concerning this problem, Fig. 6 gives next important concept: Namely, at a strain rate less than $\dot{\epsilon}_{ic}$, crack can not be initiated even though the accumulated strain exceed the minimum ductility ϵ_{ic}. This means, as a matter of course, the critical strain rate itself is a major factor determining the susceptibility in low tensile condition.

Figure 12 shows the relation between carbon content and the critical strain rate ($\dot{\epsilon}_{ic}$) required for crack initiation for tentative plain carbon steels, with the parameter of sulphur and phosphorus content. It is understood well that the change in crack susceptibility due to the increase in carbon, sulphur or phosphorus is well reflected on the reduction of ϵ_{ic}.

The behavior of $\dot{\epsilon}_{ic}$ for the stainless steels and Inconel alloy 600 is illustrated in **Fig. 13.** It is also understood that the order of crack susceptibility accepted usually is well reflected on the change in $\dot{\epsilon}_{ic}$. Therefore, under low tensile condition, sensitive index for crack susceptibilities among the materials is not ϵ_{ic} but $\dot{\epsilon}_{ic}$.

The reason why $\dot{\epsilon}_{ic}$ is a good parameter compared with

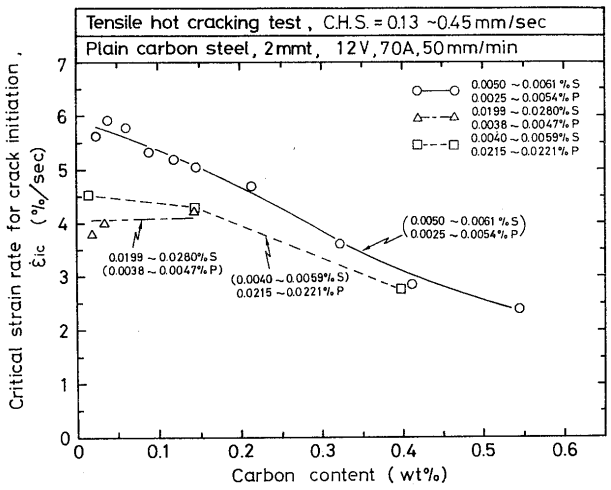

Fig. 12 Relation between carbon content and critical strain rate in plain carbon steel

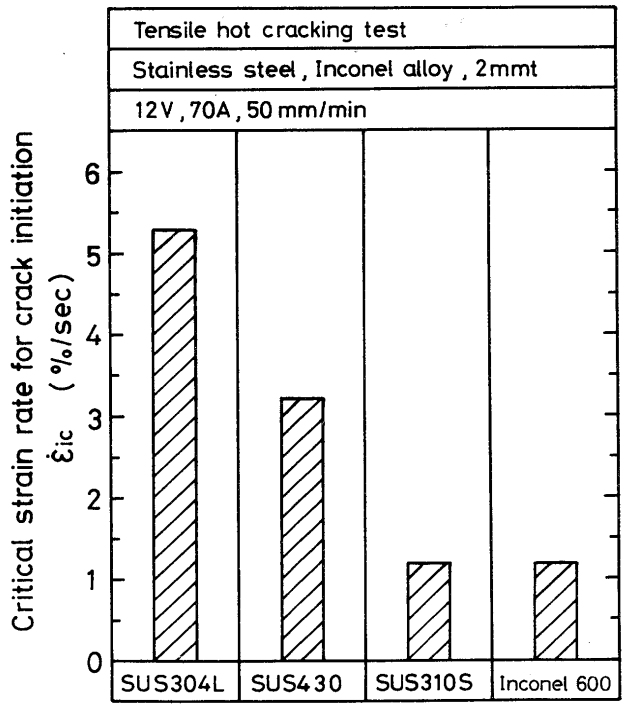

Fig. 13 Comparison of critical stain rate in stainless steels and Inconel alloy 600

ϵ_{ic} is explained as follows: Now, according to Eq. (4),

$$\dot{\epsilon}_{ic} = \epsilon_{ic} / t_{ic} \ (\%/\text{sec}) \qquad (5)$$

where t_{ic} is the lapse time when the reference points move from solidification front to the crack initiation site in the critical condition. This means that the decrease in $\dot{\epsilon}_{ic}$ is connected with the increase in t_{ic} if ϵ_{ic} is nearly constant as shown in Fig. 9. In other words, it is guessed that the t_{ic} is increased with the crack susceptibility. Thus, the relation between carbon content and t_{ic} with the parameter of sulphur and phosphorus content is shown in **Fig. 14** for tentative plain carbon steels. The behavior of t_{ic} for the stainless steels and Inconel alloy 600 is illustrated in **Fig. 15**. These correlations are just inverse

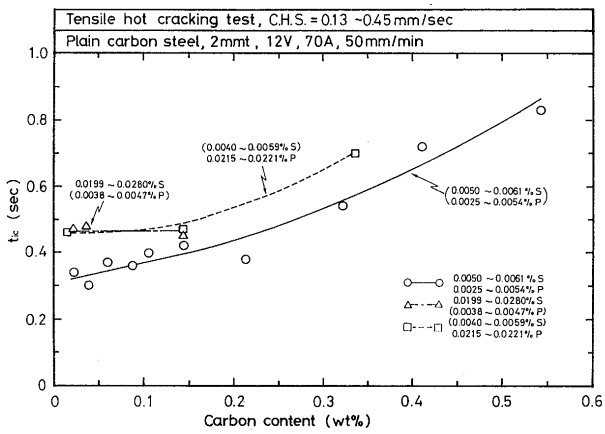

Fig. 14 Relation between carbon content and lapse time from solidification front to crack initiation t_{ic} in plain carbon steels

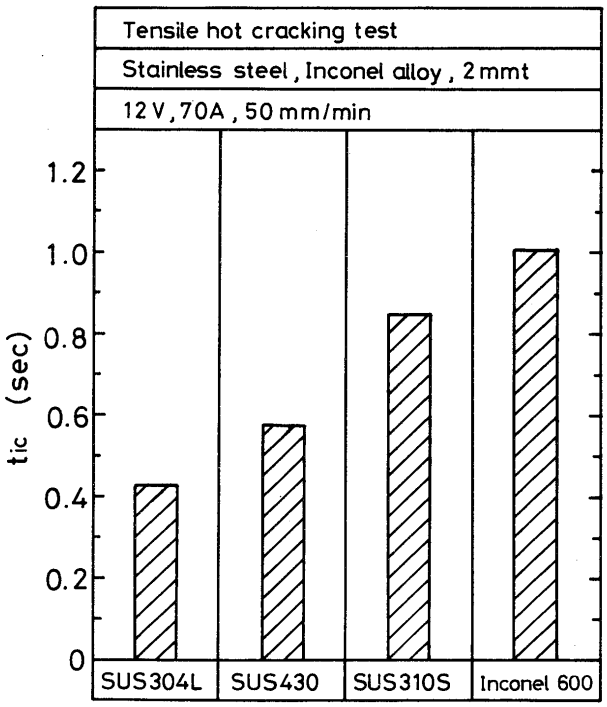

Fig. 15 Comparison of lapse time from solidification front to crack initiation t_{ic} in stainless steels and Inconel alloy 600

compared with Fig. 12 and 13, and mean the validity of the above prospect.

The increase in t_{ic} under constant temperature gradient means the large temperature difference between the solidification front and the crack initiation site. This may be interpretted as follows: The fracture surface of solidification crack is generally divided into three types depending on temperature, namely dendritic Type D in the highest temperature zone, transitional Type D-F and flat Type F in the lowest temperature zone.[9] Type D-F is considered to be the liquid film stage.[9] In accordance with this the crack initiation site measured by MISO technique is nearly located in the region of Type D-F.[10] Well, BTR increases generally together with crack susceptibility.[6] Therefore, the temperature difference from solidification front to Type D-F, namely to the crack initiation site, may have a tendency to increase together with crack susceptibility, as mentioned already.

3.3 Estimation of strain rate in welding fabrication

Figure 16 shows the increase in strain behind solidification front up to crack initiation together with lapse time for SK6 in Houldcroft-type cracking test. The gradient of increase means the strain rate under which the crack occurs in this test. The strain rate was within about 2 to 4%/sec irrespective of specimen size as shown in **Table 2(b).**

It is noteworthy that the strain rate is nearly the same as $\dot{\epsilon}_{ic}$ shown in Fig. 12 and 13, which is summarized in **Table 2(a).** Moreover, it has been shown[11] that the strain rate measured by MISO technique in a restraint cracking test by which the specimen of carbon steel is fixed at the ends through pin chucks is 1.2 to 2.2%/sec as seen in Table 2(b). Therefore, it may be concluded that the strain rate in welding fabrication, in which the deformation is considered to behave as under self-restraint condition, is nearly the same as $\dot{\epsilon}_{ic}$.

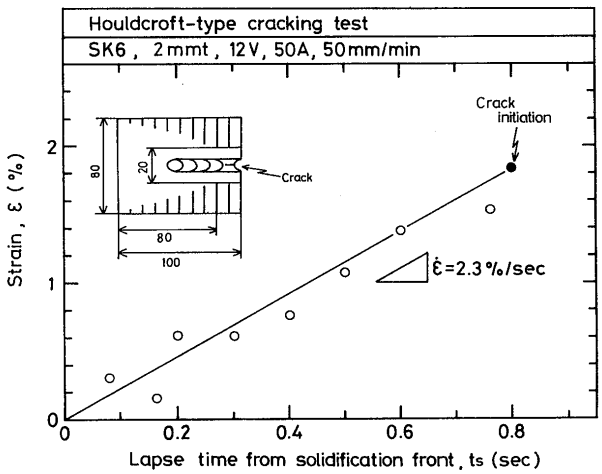

Fig. 16 An example of strain rate measured by MISO technique in Houldcroft-type cracking test

Table 2 Comparison of strain rate in different self-restraint cracking tests

(a) Critical strain rate measured by MISO technique in tensile hot cracking test

Critical strain rate $\dot{\epsilon}_{ic}$(%/sec)	Measuring method	Gauge length (mm)
2.4 ∿ 5.9	MISO	0.9 ∿ 1.7

(b) Strain rate measured by MISO technique in self-restraint cracking test

Strain rate $\dot{\epsilon}$ (%/sec)	Measuring method	Gauge length (mm)	Remark
2.1 ∿ 3.8	MISO	0.9 ∿ 1.7	Houldcroft-type cracking test
1.2 ∿ 2.2			Self-restraint cracking test [11]

(c) Strain rate estimated in Houldcroft-type cracking test

Estimated strain rate $\dot{\epsilon}$ (%/sec)	Measuring method	Gauge length (mm)
5.8×10^{-2}	Dial gauge	80

(d) Strain rate estimated in end cracking test[12–15] (One side submerged arc welding)

Estimated strain rate $\dot{\epsilon}$ (%/sec)	Measuring method	Gauge length (mm)
$1.6\sim3.3\times10^{-3}$	Dial gauge [12,13]	250 ∿ 300
$3.0\sim8.3\times10^{-3}$	Loop gauge [14]	200
7.5×10^{-2}	Calculation [15]	40

Some one, however, may claims that the strain rate in end cracking during one side submerged arc welding would be very high because the sudden remelting of tack-welded part is the cause of the cracking. In order to deny this, the strain rates in end cracking test quoted from several reference[12–15] are summarized in **Table 2(d)**. The strain rates in Table 2(b) and (d) cannot be compared with each other directly, because the gauge lengths in the end cracking tests are too large. Now, the reason why a dial gauge was set to the Houldcroft specimen as shown in Fig. 2 is to make these comparison capable. The output of dial gauge corresponds to the total deformation in W_1 in Fig. 2, where W_1 is 80 mm and thus is in nearly the same order in Table 2(d). The strain rate evaluated by the dial gauge is the mean value in the span of W_1, and gave 5.8 $\times 10^{-2}$%/sec, as shown in **Table 2(c)** which is very little compared with that by MISO technique. Comparison of this strain rate with those in Table 2(d) suggests that the strain rates in end cracking are nearly equal to or less than that in Houldcroft-type cracking test.

Therefore, it may be concluded that the strain rate in welding fabrication is in the order of critical strain rate $\dot{\epsilon}_{ic}$. Therefore, low strain rate is necessary to reveal the exact cracking phenomena. Interestingly, however, for the purpose of comparison of crack susceptibilities among materials, ϵ_{iR} evaluated in high strain rate is much better than ϵ_{ic} evaluated in the critical strain rate. In low strain rate, the critical strain rate $\dot{\epsilon}_{ic}$ itself is as excellent as ϵ_{iR}.

4. Conclusions

Effect of strain rate on the minimum ductility required for the initiation of weld solidification crack in tentative plain carbon steels, stainless steels and Inconel alloy was studied with the MISO technique combined with the tensile hot cracking test under different crosshead speeds, namely 20, 2 and 0.06 to 0.45 mm/sec. Then, the strain rate in self-restraint cracking tests including Houldcroft-type cracking test was evaluated for the estimation of that in welding fabrication. Main conclusions obtained are as follows:

(1) The minimum ductility required for crack initiation has a dependency on strain rate irrespective of materials used. That is to say, the minimum ductility is lowered with a decrease in strain rate.

(2) The degree of this dependency is related to the crack susceptibility of material. The degree is noticeable in low susceptible materials, e.g. low carbon steel, SUS304L and SUS430. It is not noticeable in high susceptible materials, e.g. low carbon steel containing high sulphur, high carbon steel, SUS310S and Inconel alloy 600.

(3) The minimum ductilities measured under the highest C.H.S. reflect well the order of crack susceptibilities accepted well among materials and the effect of harmful element such as sulphur and phosphorus. On the other hand, the minimum ductility under the lowest C.H.S. is insensitive to compare crack susceptibilities among materials.

(4) Under the low strain rate, the lower critical strain rate below which the crack can not occur is sensitive to the evaluation mentioned in (3). The effectiveness of the critical strain rate was interpreted by the term of lapse time from solidification front to the crack initiation site relating the liquid film stage in brittleness temperature range.

(5) The strain rate in self-restraint cracking tests including Houldcroft-type cracking test is as low as the critical strain rate mentioned in (4). Moreover, it was estimated that the strain rate in welding fabrication is

as low as the critical strain rate.

Acknowledgement

The authors would like to thank Mr. Shinya Kajisa, formerly student of Kinki Univ., for his cooperation in the experiment, and Nippon Steel Corporation for supply of materials.

References

1) T. Senda, F. Matsuda, et al.: "Studies on Solidification Crack Susceptibility for Weld Metals with Trans-Varestraint (2)", J. Japan Weld, Soc., Vol. 42 (1973), No. 1, pp. 48–56 (in Japanese).

2) Y. Arata, F. Matsuda et al.: "Solidification Crack Susceptibility of Aluminum Alloy Weld Metals (Report II)", Trans. of JWRI, Vol. 6 (1977), No. 1, pp. 91–104.

3) Y. Arata, F. Matsuda, et al.: "Solidification Crack Susceptibility in Weld Metals of Fully Austenitic Stainless steels (Report III)", Trans. of JWRI, Vol. 6 (1977), No. 2, pp. 37–52.

4) Y. C. Zhang, H. Nakagawa and F. Matsuda: "Weldability of Fe-36%Ni Alloy (Report III)", Trans. of JWRI, Vol. 14 (1985), No. 1, pp. 107–114.

5) F. Matsuda, H. Nakagawa, et al.: "Quantitative Evaluation of Solidification Brittleness of Weld Metal during Solidification by Means of In-Situ Observation and Measurement (Report I)", Trans. of JWRI, Vol. 12 (1983), No. 1, pp. 65–72.

6) F. Matsuda, H. Nakagawa, et al.: "Quantitative Evaluation of Solidification Brittleness of Weld Metal during Solidification by Means of In-Situ Observation and Measurement (Report II)", Trans. of JWRI, Vol. 12 (1983), No. 1, pp. 73–80.

7) K. Ando, S. Nakata, et al.: "Occurring and Developing Mechanism of Transverse Hot Cracking due to Rotational Deformation of Specimen and the Method of Assessment of Hot Cracking Susceptibility, including Criticism on Houldcroft Hot Cracking Test", J. Japan Weld. Soc., Vol. 42 (1973), No. 9, pp. 879–889 (in Japanese).

8) T. Maki and I. Tamura: "Metallurgy on Hot Working of Steel", Bulletin of Japan Inst. Metals, Vol. 19 (1980), No. 2, pp. 59–63 (in Japanese).

9) F. Matsuda and H. Nakagawa: "Fractographic Investigation on Solidification Crack in the Varestraint Test of Fully Austenitic Stainless Steel", Trans. of JWRI, Vol. 7 (1978), No. 1, pp. 59–70.

10) To be published.

11) To be published.

12) Y. Fujita, et al.: "Prevention of End Cracking in One Side Automatic Welding (1st Report)", Soc. Naval Arch. Japan, 133 (1973), pp. 267–275 (in Japanese).

13) N. Okuda and K. Tanak: "Mechanism and Prevention of the End Crack in One Side Submerged Arc Welding (Report 2)", J. Japan Weld. Soc., Vol. 51 (1982), No. 5, pp. 423–429 (in Japanese).

14) T. Maeda, et al.: "One the Prevention of End Cracking in One Side Welding (1st Report)", Soc. Naval Arch. Japan, 129 (1971), pp. 167–177 (in Japanese).

15) Y. Fujita, et al.: "Studies on Prevention of End Cracking in One Side Automatic Welding (2nd Report)", Soc. Naval Arch. Japan, 135 (1974), pp. 379–391 (in Japanese).